Proprioceptive State Estimation for Legged Robots without Contact Sensing using Hybrid Factor Graphs

Author Names Omitted for Anonymous Review

***Abstract*—Proprioceptive state estimation is a critical capability for legged robots, enabling feedback control in challenging environments where exteroceptive sensing may be unreliable or unavailable. A common component of proprioceptive estimation pipelines is discrete foot contact sensing, which allows kinematic constraints to be imposed on the system state. However, contact sensors are often brittle and prone to failure in real–world deployments, motivating the need for alternative methods to infer foot contact. In this work, we represent this hybrid problem of simultaneously estimating the continuous base state of a legged robot and the discrete contact states of its feet as a hybrid factor graph, using only proprioceptive measurements from a base–mounted IMU and joint encoders and without any force/torque sensor measurements. Our key insight is that IMU–observed motions on legged robots are more physically consistent when a foot is in contact with the ground. We encode this insight through a novel discrete–continuous contact factor within a hybrid factor graph, which enables representation and joint inference over continuous states and discrete modes in a principled probabilistic framework. We validate our approach through both simulation and hardware experiments, demonstrating accurate state estimation using only proprioceptive kinematic and inertial measurements. Across platforms, our estimator achieves greater than 83% contact detection accuracy while maintaining state estimation performance comparable to contact–aware methods, without using any dedicated contact sensing. The proposed framework is platform–agnostic and readily extensible to additional sensing modalities via new factors, opening avenues for contact estimation beyond traditional legged robot state estimation pipelines.**

I. Introduction

Proprioceptive state estimation is an important capability for legged robots to be able to operate in all manner of environments. Legged robots are expected to perform not only in well-structured urban environments, but also underground passages, debris filled areas, *etc*., scenarios where exteroceptive sensing may not be accurate or even feasible [27].

An important component of proprioceptive legged robot state estimation is the ability to measure the contact state of the legs. If the leg is in contact, the corresponding leg kinematics can be leveraged to constrain the base Inertial Measurement Unit (IMU) measurements and obtain accurate state estimates. However, foot contact sensors have major drawbacks, *e.g*. they are noisy, have time delays, break easily during long-term operation, and are not available on all robots, thus necessitating the need for estimating contact. Additionally, we would also like to be able to update the previously incorrect contact measurements based on new information.

In this paper, we propose an approach for proprioceptive state estimation of a legged robot in the absence of dedicated contact sensing, by jointly inferring the foot contact state using only kinematic measurements (*i.e*. the base IMU and joint encoders). We do so without the need for dedicated contact and/or force/torque sensors or additional hardware (*e.g*. leg IMUs), thus alleviating the cost and complexity associated with these approaches. Since the ability to estimate the continuous state and the discrete contact sequence for each leg is a hybrid estimation problem, we represent our state estimator as a hybrid factor graph [1]. Based on the insight that IMU-observed motions are physically consistent with alternating leg contact with the ground, we develop a novel hybrid leg contact factor which connects the continuous foot odometry with the discrete contact states to represent different leg phases. We also represent each foot's contact state over time as a Markov chain connected by discrete transition factors, with the transition matrix computed from either annotated data or the contact schedule. Our method allows us to estimate the discrete contact state simultaneously along-with the continuous state using only proprioceptive and kinematic measurements, alleviating the aforementioned issues with contact sensing. Moreover, our algorithm is general and can be applied to any robot with an arbitrary number of legs and is easy to extend with more contact states such as slip, as well as scenarios beyond legged robots, e.g. grasping.

To validate our approach, we compare our results against Discrete-Continuous Smoothing and Mapping (DCSAM) [11] since it allows us to make perform a fair comparison under the same measurement sets. We leave comparison with observer-based [10] and filtering-based [17] estimators which require force-torque sensing for future work.

II. Related Work

To estimate continuous states as well as discrete contacts, previous approaches have tackled this in a variety of ways. Importantly, these approaches generally tackle the contact estimation problem separately from the state estimation problem, and we discuss these problems separately below as well.

Proprioceptive state estimation for legged robots has recently been widely studied in the literature. The line of work from Bloesch *et al*. first established the major paradigm of Kinematic-Inertial Odometry (KIO) for legged robots [5, 4, 6]. Follow up works have introduced new methods and approaches to improve the accuracy. Hartley *et al*. [14, 13] develop new contact preintegration factors to better model the transition of the foot contact. Agrawal et al. [2] and Yang et al. [30] propose approaches to handle leg link deflections, while Ramadoss et al. [24] and Teng et al. [26] leverage the $\mathrm{SE}_2(3)$ Lie group and the Invariant EKF with a camera respectively to better capture the velocities of the base and the feet. Santana et al.

[25] leverages robust cost functions to handle outliers in the measurement update process of an Invariant Extended Kalman Filter (InEKF). Both Yang et al. [31] and Wu et al. [28] make use of multiple additional IMUs to perform proprioceptive state estimation for legged robots.

One of the earlier works used to tackle contact classification for legged robots was by Camurri et al. [8]. By using Recursive Newton Euler Algorithms to compute the ground reaction force (GRF), a linear regression model is employed to classify the contact state. In a similar vein, Hwangbo et al. [16] develop a discrete Hidden Markov Model using information from the robot dynamics and differential kinematics to perform probabilistic contact classification. Lin et al. [18] and Piperakis et al. [23] use (deep) learning based approaches to classify contact events using proprioceptive information from the robot, while Youm et al. [32] develop a Neural Measurement Network to estimate the base linear velocity and foot contact probabilities to inform an InEKF based state estimator. An alternate approach for contact estimation involving the use of extra IMUs on the robot legs is proposed by Maravgakis et al. [19], who use a Kernel Density Estimator on the leg IMU measurements to estimate contact. However, this involves hardware modifications to the robot, since the large majority of currently available robots don't have these leg IMUs available.

The work from Doherty et al. [11] and Menner and Berntorp [20] are contemporary approaches which perform hybrid state estimation. Menner and Berntorp [20] leverages the Interacting Multiple Model Kalman Filter [7] framework to perform state and contact estimation simultaneously, but suffer from relinearization errors. Doherty et al. [11] also uses a hybrid factor graph but performs optimization in an alternating scheme over continuous and discrete variables, fixing the values of the other, which makes it prone to getting stuck in local minima.

III. Preliminaries

A. Hybrid Factor Graph

A factor graph is a probabilistic graphical model with a bipartite structure $\Phi = \{\phi, \mathcal{V}, \mathcal{E}\}$. The variables $\mathcal{V}$ are connected to factors ϕ via edges $\mathcal{E}$.

If the variables in a factor graph can take on either discrete or continuous values, we denote it as a **hybrid factor graph**. The hybrid factor graph represents the joint probability distribution of the continuous variables X and the discrete variables M given measurements (or evidence) Z, which factorizes as

$$P(X, M|Z) \propto \prod_{i=1}^{\Phi} \phi_i(X_i, M_i; Z_i) \tag{1}$$

Any factor within this graph which has edges to both discrete and continuous variables is a hybrid factor ϕ^H. Otherwise, if the factor is only connected to continuous (discrete) variables, it represents a continuous (discrete) factor ϕ^C (ϕ^D).

$$\begin{aligned} &\phi^H(X_k, M_k) \propto P(Z_k|X_k, M_k) \vee P(X_k|M_k) \\ &\phi^C \propto P(Z_k|X_k) \vee P(X_k) \\ &\phi^D \propto P(Z_k|M_k) \vee P(M_k) \end{aligned} \tag{2}$$

B. Hybrid Variable Elimination

We perform variable elimination on a hybrid factor graph to convert it to a **hybrid Bayes network** $P(X, M|Z)$ [1], which can be optimized to estimate the *Maximum A Posteriori* values of X, M. By performing elimination of continuous variables before any discrete variables (*a.k.a.* a strong ordering [21]), the hybrid Bayes network takes on a tree structure with each non-leaf node representing a discrete variable $m_i \in M$ and the leaves form the continuous conditional distribution given a discrete assignment $P(X|M, Z)$. This has the advantage of giving us an exact posteriori value without any approximations. To maintain tractability as the tree grows with the number of variables, pruning and dead mode removal are performed [1].

IV. Methodology

A. Hybrid Legged Robot State Estimation

We are interested in simultaneous proprioceptive state and contact estimation for legged robots using only measurements from the IMU and the joint encoders on the legs. Since legged robots perform switching contact with their environment, the contact state of each foot forms the discrete variables while the pose and velocity of the robot forms the continuous aspect. It is important to note that our approach is general and can be applied to all types of legged robots.

We define the hybrid state of a legged robot at discrete timestep k as

$$\boldsymbol{H} = \{X_B^A, M\}_k \tag{3}$$

Here, $X_B^A = \{R_B^A, p_A, v_A, b\}$ is the continuous robot state, with R_B^A as the rotation of the base of the robot with respect to some fixed inertial frame A, p_A and v_A are the translation and linear velocity respectively of the robot base in frame A, and b is the 6D gyroscope and accelerometer bias of the IMU in the sensor frame which is jointly estimated. The angular velocity of the robot can be directly measured from the IMU mounted on the robot base. The discrete state of the robot is given by $M = \{M_f; f \in N\}$ where $M_f \in \{0, 1\}$ is the contact state of leg f, with 1 representing contact and 0 representing no-contact, and N is the number of legs. While we only model binary contact states currently, our methodology allows for additional states, such as slip, which we leave for future work.

We build on the proprioceptive state estimation framework proposed in [2] to develop our hybrid estimator. For the continuous state estimator, given the IMU's gyroscope and accelerometer measurements $\{\omega, a\}$, we correct for the bias drift by leveraging the switching ground contact of the legs using joint encoder measurements $\boldsymbol{J}$, performing sensor fusion for state estimation [5]. Since our framework doesn't require contact sensing, our measurements at timestep k are:

$$Z_k = \{\omega, a, \boldsymbol{J}\}_k \tag{4}$$

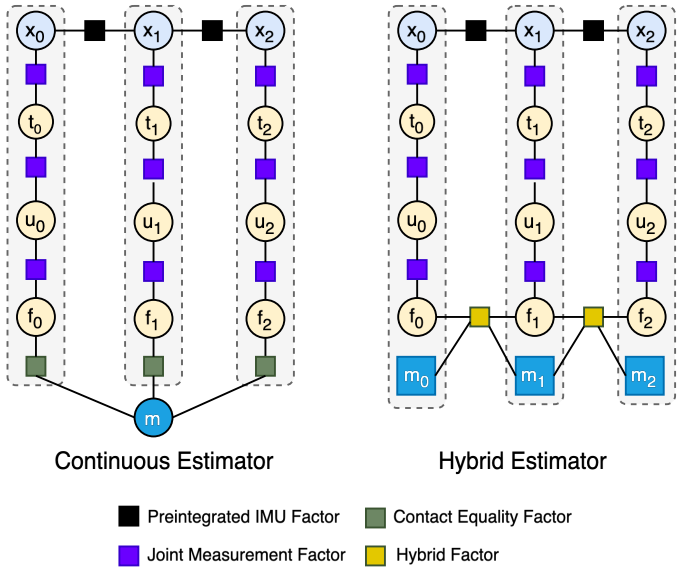

Fig. 1: Factor graph representations of the continuous state estimator [2] (left) and our proposed hybrid state estimator (right), for a single leg over 3 timesteps. x represents the robot base state, and f is the foot link of the robot. m is the discrete mode {no-contact, contact} the foot is in.

B. Hybrid Factor Graph

To perform hybrid state estimation, we use the hybrid factor graph described in [1] and provide details for the factor graph structure here. Given the factor graph for proprioceptive state estimation described in [2], a few simple changes allow us to convert it to a hybrid graph.

The hybrid factor graph for a single leg with measurements over two timesteps $k, k+1$ has the following structure:

$$\begin{aligned}\Phi =& \phi_{\text{IMU}}(x_k, x_{k+1}; \omega, a) \\ & \phi_{\text{FK}}(x_k, t_k; \boldsymbol{J}_k^t)\phi_{\text{FK}}(t_k, u_k; \boldsymbol{J}_k^u)\phi_{\text{FK}}(u_k, f_i; \boldsymbol{J}_k^f) \\ & \phi_{\text{FK}}(x_{k+1}, t_{k+1}; \boldsymbol{J}_{k+1}^t)\phi_{\text{FK}}(t_{k+1}, u_{k+1}; \boldsymbol{J}_{k+1}^u) \\ & \phi_{\text{FK}}(u_{k+1}, f_{k+1}; \boldsymbol{J}_{k+1}^f) \\ & \phi_{\text{hybrid}}(f_k, f_{k+1}, m_k, m_{k+1})\end{aligned} \tag{5}$$

Here, $x = \{R_B^A, p_A, v_A, b\}$ represents the continuous state estimate vector, t, u, f are the links in the kinematic chain of the leg, as depicted in Fig. 1, and $\boldsymbol{J}$ are the joint encoder measurements with the superscript specifying the joint index. ϕ_{IMU} represents the IMU preintegration factor, and ϕ_{FK} is a factor for the relative pose between two connected links given the joint angle measurement *a.k.a.* the forward kinematics.

We replace the *Contact Point* factor used in [2] with a *Hybrid Contact Factor* ϕ_{hybrid} connecting the continuous feet and the discrete contact variables, which we describe in more detail in IV-C. For each timestep k the IMU preintegration factor is added, we also add the joint measurement factors for the legs, and use the hybrid contact factor to connect the continuous foot and discrete contact variables at k with the ones at the previous timestep $k-1$.

C. Hybrid Contact Factor

We use a hybrid nonlinear factor in our estimator for each leg f to model the relationship between the foot and its contact state at consecutive timesteps $i, i{+}1$. The hybrid factor consists of a set of $|M_f|^{|\{i,i+1\}|}$ nonlinear factors, each indexed by the assignment of $\{m_i, m_{i+1}\} \in M_f$. Since we model binary contact, each discrete variable m has a cardinality of 2, which for 2 consecutive timesteps gives the hybrid contact factor $2^2 = 4$ nonlinear components. Each component corresponds to a different leg phase model, and thus the hybrid factor tracks 4 different hypotheses: swing, lift, land and stance.

m_i	m_{i+1}	**Nonlinear Factor**	**Foot Displacement (Phase)**
0	0	$\phi_{00}(f_i, f_{i+1})$	High (Swing)
0	1	$\phi_{01}(f_i, f_{i+1})$	Intermediate (Land)
1	0	$\phi_{10}(f_i, f_{i+1})$	Intermediate (Lift)
1	1	$\phi_{11}(f_i, f_{i+1})$	Small (Stance)

Mathematically, the hybrid factor is defined as

$$\phi_{\text{hybrid}}(f_i, f_{i+1}, m_i, m_{i+1}) = \begin{cases} \phi_{00}(f_i, f_{i+1}) & \text{if } m_i = 0, m_{i+1} = 0 \\ \phi_{01}(f_i, f_{i+1}) & \text{if } m_i = 0, m_{i+1} = 1 \\ \phi_{10}(f_i, f_{i+1}) & \text{if } m_i = 1, m_{i+1} = 0 \\ \phi_{11}(f_i, f_{i+1}) & \text{if } m_i = 1, m_{i+1} = 1 \end{cases} \tag{6}$$

with each factor's error function being

$$\begin{aligned}\phi_{m_i m_{i+1}}(f_i, f_{i+1}) = \\ \|\text{g}(f_{i+1}) - \text{g}(f_i) - \mu_{m_i m_{i+1}}\|^2_{\Sigma_{m_i m_{i+1}}}\end{aligned} \tag{7}$$

where $g : \text{SE}(3) \to \mathbb{R}^3$ computes a point on a robot's link relative to the pose of the Center-of-Mass of that link, e.g. the contact point of the foot link on a quadruped, and $\mu_{m_i m_{i+1}}$ and $\Sigma_{m_i m_{i+1}}$ are the mean and the covariance respectively.

For our purposes, we model the hybrid contact factor with differing covariances for each phase. Our insight is that for the stance phase, *i.e.* the foot is in contact across two timesteps, we can use a tighter covariance bound around the position of the foot versus a looser covariance bound for the other phases when the foot is not constrained to be in the same position.

To concretely model the hybrid factor, we leverage a Contact Equality factor, defined as:

$$\phi^{\text{CE}}_{m_i m_{i+1}}(f_k, f_{k+1}) = \|g(f_{k+1}) - g(f_k)\|^2_{\Sigma_{\text{CE}}} \tag{8}$$

with Σ_{CE} as the covariance matrix, giving us:

$$\phi_{\text{hybrid}}(f_i, f_{i+1}, m_i, m_{i+1}) = \begin{cases} \phi^{\text{CE-swing}}_{m_i m_{i+1}}(f_i, f_{i+1}) & \text{if } m_i = 0, m_{i+1} = 0 \\ \phi^{\text{CE-land}}_{m_i m_{i+1}}(f_i, f_{i+1}) & \text{if } m_i = 0, m_{i+1} = 1 \\ \phi^{\text{CE-lift}}_{m_i m_{i+1}}(f_i, f_{i+1}) & \text{if } m_i = 1, m_{i+1} = 0 \\ \phi^{\text{CE-stance}}_{m_i m_{i+1}}(f_i, f_{i+1}) & \text{if } m_i = 1, m_{i+1} = 1 \end{cases} \tag{9}$$

In our experiments, we use the same covariance values for swing, land, and lift to model larger variations between the position of the foot contact point.

To linearize the hybrid factor, we need to linearize each of the component factors using a Taylor expansion. This involves computing the Jacobians S_i, S_{i+1} of each component factor with respect to the continuous variables f_i, f_{i+1} respectively.

$$S_i^{m,m+1} = \frac{\partial \phi_{m,m+1}^{\text{CE}}}{\partial f_i} \tag{10}$$

$$S_{i+1}^{m,m+1} = \frac{\partial \phi_{m,m+1}^{\text{CE}}}{\partial f_{i+1}} \tag{11}$$

$$d^{m,m+1} = \phi_{m,m+1}^{\text{CE}}(f_i, f_{i+1}) \tag{12}$$

where d is the error state vector. We leverage the continuous factor definition to compute these values for each mode assignment $m, m+1$, and numerically verify correctness.

D. Discrete Transition Factor

Additionally, we can also add a discrete factor representing the transition between two estimated foot states. Similar to a Markov chain, the transition factor represents the transition probability of each foot from one timestep to the next.

Since the foot can be in contact or no-contact, there are 4 possible transitions $(00, 01, 10, 11)$, representing swing, land, lift, and stance phase. The transition probabilities can be numerically estimated if we have a small dataset of recorded foot contact, such as from our simulation, or the controller's contact schedule. These computations are done on a per foot basis in order to better accurately model the gait of the robot.

An important aspect to note is that we compute transitions at the estimation rate and not for successive timesteps. This is because we wish to represent the transition probability between successive estimated foot states, the interval rate of which might be greater than the data rate, *e.g.* for an estimation rate of 50 Hz with a simulation rate of 250 Hz, we need to estimate transition probabilities for every 5th step.

V. State Estimation Experiments

We evaluate our proposed state estimator using data collected from both simulation and hardware. For collecting simulation data, we use Mujoco Playground [33] as it provides us with the necessary infrastructure to run locomotion policies for both the Go1 quadruped and the G1 humanoid. For validation on hardware, we use the data collected from an ANYbotics ANYmal C quadruped by the Dynamic Robot Systems Group at the University of Oxford.

When optimizing our hybrid estimator, to maintain tractability we prune the discrete tree in the hybrid Bayes network to a maximum of 16 leaves and set the dead mode removal threshold to $\delta_{\text{DMR}} = 0.99$.

A. Simulated Humanoid

We use the Unitree G1 human for simulation experiments since it is highly ubiquitous given its low-cost and ease of programmability. It has thus seen wide adoption in the reinforcement learning and whole body control community [9, 15, 29]. To address the need for state estimation on this humanoid, we present the below results, with qantitative results provided in Table I and qualitative results in Fig. 3. In particular, we examine three scenarios:

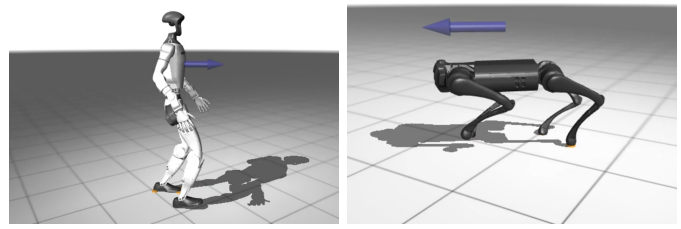

Fig. 2: The G1 and Go1 robots walking in simulation in the MuJoCo environment.

- Ground truth contact provided, which serves as a continuous-only state estimation baseline.
- With noisy contact measurements, which allows us to examine the benefits of using a hybrid probabilistic scheme, and the effect of continuous variables on the discrete variables.
- No contact measurements, which requires the estimator to classify contact using purely kinematic information.

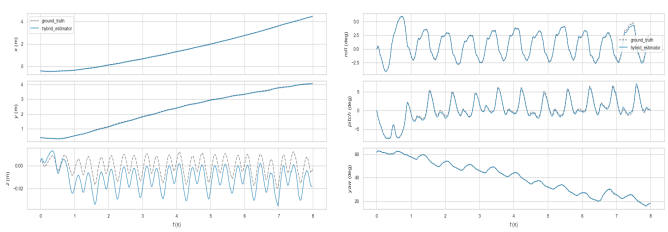

Fig. 3: Continuous state estimates of the G1 robot.

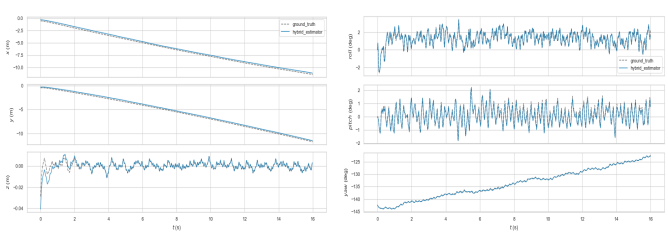

Fig. 4: Continuous state estimates of the Go1 robot.

The results in Table I allow us to conclude that our estimator is capable of leveraging the kinematics information to identify contact and provide accurate continuous state estimates, marking a significant improvement over current state of the art which requires additional sensing such as force-torque or Ground Reaction Force computation. Most importantly though, due to the use of a hybrid factor graph, extending our estimator with force-torque measurements is straightforward and something we intend to examine in future work.

TABLE I: RMSE on ASE, APE and RPE for the G1 humanoid and Go1 quadruped with true contacts, and no contact measurements provided.

Robot	Contacts Provided	ASE	APE	RPE
Quadruped	True Contacts	0.60545	0.53558	0.00576
	No Measurements	1.09767	1.04848	0.15571
Humanoid	True Contacts	0.84684	0.13047	0.00418
	No Measurements	0.97586	0.46545	0.03563

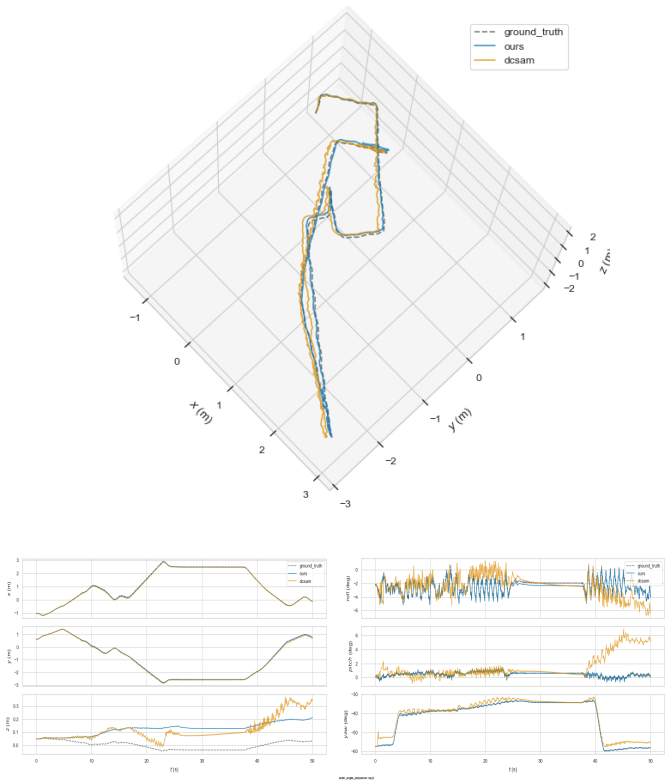

Fig. 5: State estimate results of our hybrid estimator on a trajectory of the ANYmal C quadruped. Results from DCSAM [11] are also provided for comparison.

B. Simulated Quadruped

Similar to the G1, the Go1 is also a ubiquitous quadruped, and thus we demonstrate our estimator's efficacy on this platform. Quantitative results are provided in Table I and qualitative results can be seen in Fig. 4.

C. Hardware

Here we present results of our hybrid state estimator on trajectory data collected from a ANYmal C robot in hardware. The robot trajectories are each over 15 meters long, and performing various motions, including loops. Ground truth trajectory data is captured using a Vicon motion capture system. Importantly, the ANYmal C robot has contact sensors installed in its feet, thus providing us with ground truth foot contact information which we use to compare our foot contact estimates against. Thus, the sensor measurements include foot contacts alongwith the robot base IMU and the joint angles.

As a comparative baseline, we use DCSAM [11] to optimize our hybrid factor graph. We limit ourselves to DCSAM since other proprioceptive state estimators rely on some form of additional sensing (*e.g.* IMUs on the feet, force-torque sensors) to estimate foot contact, which our estimator doesn't need.

We show quantitative results in Table II and qualitative results in Fig. 5. Our hybrid estimator is able to outperform DCSAM while achieving a contact accuracy of $\approx 87\%$ (which is further discussed in section VI). This experiment validates that our approach is able to accurately estimate both the continuous state and the discrete contact simultaneously.

TABLE II: RMSE on ASE, APE and RPE metrics for ANYmal C hardware data. We compute these for our hybrid state estimator as well as DCSAM to compare the performance.

Trajectory	Estimator	ASE	APE	RPE
Trajectory 1	Ours	**0.9233**	**0.7487**	**0.1410**
	DCSAM	1.4810	0.9334	0.2178
Trajectory 2	Ours	**0.2455**	**0.2398**	**0.0471**
	DCSAM	0.2503	0.2441	0.0472

VI. Contact Estimation Experiments

In this section, we analyze the contact estimate accuracy of our hybrid state estimator under varying degrees of noise via Monte Carlo simulations. Due to its probabilistic nature, the hybrid factor graph can additionally have measurement factors on the discrete variables, with discrete mass functions modeling the accuracy of the contact sensor/sensing algorithm.

A. Types of Contact Measurements Provided

We demonstrate via experiments performed on simulated data how our hybrid estimator is able to account for contact measurements, and overcome potential noise in them. Using the Go1 quadruped and the G1 humanoid in simulation, we collect trajectory data including the ground truth contact states. These contact states are provided to the estimator in 3 ways:

1) True Contacts: In this experiment, we provide the estimator with the true contact values. By doing this, we simplify the hybrid estimation problem to a continuous state estimation problem, similar to [2]. This provides us with a strong performance ceiling on which to establish the accuracy of our estimator, and verify its operational success.

2) Noisy Contact Measurements: We provide the hybrid state estimator with noisy contact measurements. Using either a noisy/low quality contact sensor or an algorithmic approach (such as sampling) we can obtain potentially noisy contact measurements which can be probabilistically fused. To corrupt the contact measurements with noise, we sample the contacts Z from a custom defined distribution $P(Z|C)$ conditioned on the true contact C.

3) No Contact Measurements: In this scenario, no contact measurements are provided, and our hybrid estimator is tasked with estimating the contact state from only the kinematics. This is a harder problem, yet we see our estimator is able to provide $> 80\%$ accuracy for contact classification.

While (1) is trivial and reduces to a continuous-only estimator, (2) and (3) demonstrate the strengths of our approach to probabilistically fuse these discrete measurements along with the continuous ones.

Finally, we report on the contact accuracy of our hybrid estimator on ANYmal C hardware. We use the contact sensor on the ANYmal C as our "ground truth" contacts.

B. Quadruped Simulation

We first perform our analyses on the Go1 quadruped. Due to the larger number of legs on the Go1 quadruped compared to, for example a humanoid, there exists a higher rate of failure due to incorrect contact classification. These experiments thus provide us with a strong demonstration of both the accuracy and efficiency of our hybrid estimator.

TABLE III: Foot contact accuracy for contact estimation from our hybrid estimator. The simulated contact sensor is modeled to provide "Noisy measurements" (with 75% sampling accuracy). With these noisy measurements, our estimator is able to recover the "Estimated" contacts with $> 90\%$ accuracy. For "No measurements", our estimator is not given contact measurements, using only the inertial + kinematics measurements to estimate contact .

Robot	Foot	Noisy Meas.	Estimated	No Meas.
Go1 Quadruped	Front Right	68.875%	94.375%	88.25%
	Front Left	67.375%	93.375%	81.00%
	Rear Right	69.625%	95.875%	84.50%
	Rear Left	69.50%	90.25%	80.25%
G1 Humanoid	Left	75.75%	90.50%	84.50%
	Right	77.50%	94.25%	90.75%

From Table III, we can see that hybrid estimator is able to improve contact classification by over 15% compared to the accuracy of the noisy sensor. We see similar results for when no contact measurements are provided, highlighting that probabilistically incorporating kinematic information into the contact classification process allows for better estimation.

TABLE IV: Foot contact accuracy at different levels of contact sensor accuracy (75%, 50%, and 25%) represented as the sampling probabilities.

Robot	Foot	P(0.75)	P(0.5)	P(0.25)
Go1 Quadruped	Front Right	94.375%	85.375%	85.625%
	Front Left	93.375%	77.875%	83.25%
	Rear Right	95.875%	85.25%	76.125%
	Rear Left	90.25%	77.625%	71.75%
G1 Humanoid	Left	90.50%	89.50%	78.00%
	Right	94.25%	89.50%	76.75%

To verify the robustness of our hybrid estimator, we analyze the contact classifications over different sensor noise levels corresponding to the probabilities $\{0.75, 0.5, 0.25\}$. The estimator's contact classification accuracy is presented in Table IV. We note that our estimator is able to consistently classify contact with $\approx 80\%$ accuracy even despite noisy sensors. This is an encouraging result, since it demonstrates the robustness and efficacy of our estimator over diverse terrains.

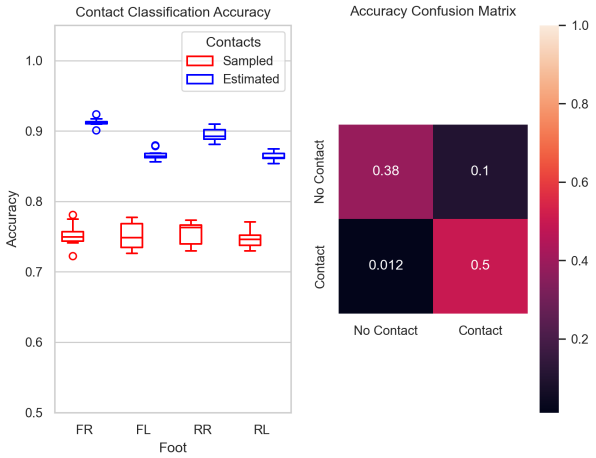

Fig. 6: Contact estimation accuracy for the Go1 quadruped. The box-plot shows the accuracy mean and standard deviation of the estimated contacts versus the noisy contact measurements for each foot. The confusion matrix illustrates the overall classification accuracy of our contact estimation.

Finally, we wish to understand the variance of our estimates over different runs of the robot. To do so, we sample the contacts using 10 different random seeds to generate 10 separate contact trajectories. We run our estimator on each of the trajectories and aggregate the means and standard deviations for each foot. As a baseline, we also include the plot of the mean classification accuracy and standard deviations for the raw sampled contacts in 6. Note that for the raw sampled contacts, the accuracies of the feet on the right side are lower. This is primarily due to the gait of the robot being generated by the reinforcement learning policy used.

C. Humanoid Simulation

In this section, we run similar experiments on the G1 humanoid, showcasing our estimator's efficacy as evidenced in Table III. We similarly evaluate the robustness of contact classification against different levels of contact sensor noise, following the same sampling protocol as in the quadruped case. The contact classification accuracy is reported in Table IV, where we see that despite increasing contact sensor noise levels, our estimator is able to consistently estimate $> 83\%$ contact accuracy. We also perform a multi-run variance evaluation of our G1 contact estimates. Fig. 7 shows that our estimator computes higher contact accuracies with lower standard deviations.

D. Hardware

We further validate the accuracy of our estimator's contact classification using the ANYmal C quadruped as our hardware platform. Quantitative results are presented in Table V.

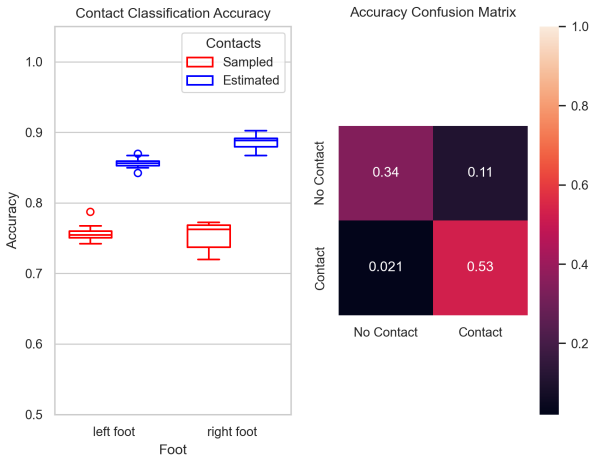

Fig. 7: Contact estimation accuracy for the G1 humanoid (similar to the Go1).

TABLE V: Foot contact accuracy for contact estimation from our hybrid estimator on ANYmal C hardware. We use the contact sensor measurements as the "ground truth".

Trajectory	Front Right	Front Left	Rear Right	Rear Left
Trajectory 1	84.486%	83.846%	83.646%	84.806%
Trajectory 2	86.414%	85.215%	85.115%	86.314%

E. Discrete Transition Factor

Finally, we present experimental results on the use of our proposed discrete transition factor between foot state variables in the hybrid factor graph. This factor behaves similarly to the transition function in a Markov chain, and its values can be estimated directly from the data. In our case, we used the true contacts obtained from the simulation, but contact schedules provided to controllers can also be used.

TABLE VI: Absolute State Error RMSE for the Go1 quadruped, the G1 humanoid and the ANYmal C, without and with the discrete transition factor. Lower values are better.

Robot	Baseline	With Transition Factor
Go1 Quadruped	1.09439	**1.08218**
G1 Humanoid	0.97586	**0.97108**
ANYmal C (hardware)	0.92333	**0.90251**

We update our estimator by adding the transition factors between each two successive foot variables, and compare contact accuracies with the version without this factor. For the simulations of the Go1 quadruped and the G1 humanoid simulations as well as the ANYmal C quadruped hardware, results are presented in Table VII. We see consistent improvements in overall contact classification accuracy across all platforms when adding the discrete transition factors.

TABLE VII: Foot contact accuracy results for the Go1 quadruped, the G1 humanoid, and the ANYmal C hardware platform, without and with using discrete transition factors.

Robot	Foot	Baseline	With Transition Factor
Go1 Quadruped	Front Left	81.00%	**92.625%**
	Rear Left	80.25%	**90.75%**
	Front Right	88.25%	**95.50%**
	Rear Right	84.50%	**94.375%**
G1 Humanoid	Left	83.75%	**85.75%**
	Right	85.75%	**87.25%**
ANYmal C	Front Right	84.486%	**88.245%**
	Front Left	83.846%	**87.445%**
	Rear Right	83.646%	**88.445%**
	Rear Left	84.806%	**87.365%**

VII. Conclusion

In this work, we developed a hybrid proprioceptive state estimator for legged robots using a hybrid factor graph as the underlying framework. Our hybrid estimator is capable of simultaneously estimating the continuous state as well as the discrete contact values for each of the legs. Importantly, our estimator doesn't require the use of complex robot dynamics, additional hardware or expensive data collection, using only the base IMU and the joint encoder measurements.

We have demonstrated the efficacy of our estimator in both simulation and on hardware. Our approach compares favorably to DCSAM, a state-of-the-art inference system over hybrid factor graphs. Crucially, we are able to classify contact with over 83% accuracy, which leads to lower ASE, APE, and RPE errors compared to using noisy/no contact measurements.

One limitation of our work is the lack of additional comparisons with other contact estimation methods (using momentum observers or additional hardware) used in proprioceptive legged robot state estimation. This is because we make no assumptions about the availability of additional sensing (such as force/torque sensors and leg IMUs).

While the continuous errors of our hybrid estimator is low, there is still a significant gap to the continuous-only estimator, which can be potentially addressed by incorporating additional sources of information, such as joint torques and ground reaction forces. The probabilistic nature of our estimator provides straightforward addition of these information sources as new factors. Exploring the benefits of these additional proprioceptive sensor modalities is an interesting future direction we hope to investigate.

References

[1] Varun Agrawal and Frank Dellaert. Variable Elimination in Hybrid Factor Graphs for Discrete-Continuous Inference & Estimation, 2026. URL https://arxiv.org/abs/2601.00545.

[2] Varun Agrawal, Sylvain Bertrand, Robert Griffin, and Frank Dellaert. Proprioceptive State Estimation of Legged Robots with Kinematic Chain Modeling. In

2022 IEEE-RAS 21st International Conference on Humanoid Robots (Humanoids), pages 178–185, 2022. doi: 10.1109/Humanoids53995.2022.10000099.

[3] Gerardo Bledt, Patrick M. Wensing, Sam Ingersoll, and Sangbae Kim. Contact Model Fusion for Event-Based Locomotion in Unstructured Terrains. In *2018 IEEE International Conference on Robotics and Automation (ICRA)*, pages 4399–4406, 2018. doi: 10.1109/ICRA.2018.8460904.

[4] M. Bloesch, C. Gehring, P. Fankhauser, M. Hutter, M. A. Hoepflinger, and R. Siegwart. State estimation for legged robots on unstable and slippery terrain. In *2013 IEEE/RSJ International Conference on Intelligent Robots and Systems*, pages 6058–6064, 2013. doi: 10.1109/IROS.2013.6697236.

[5] M. Bloesch, M. Hutter, M. Hoepflinger, S. Leutenegger, C. Gehring, C. D. Remy, and R. Siegwart. *State Estimation for Legged Robots: Consistent Fusion of Leg Kinematics and IMU*, pages 17–24. IEEE, 2013.

[6] Michael Bloesch, Michael Burri, Hannes Sommer, Roland Siegwart, and Marco Hutter. The Two-State Implicit Filter - Recursive Estimation for Mobile Robots. *IEEE Robotics and Automation Letters*, 3(1):573–580, 2017. ISSN 2377-3766. doi: 10.1109/LRA.2017.2776340.

[7] H.A.P. Blom and Y. Bar-Shalom. The interacting multiple model algorithm for systems with Markovian switching coefficients. *IEEE Transactions on Automatic Control*, 33(8):780–783, Aug./1988. ISSN 00189286. doi: 10.1109/9.1299.

[8] Marco Camurri, Maurice Fallon, Stéphane Bazeille, Andreea Radulescu, Victor Barasuol, Darwin G Caldwell, and Claudio Semini. Probabilistic contact estimation and impact detection for state estimation of quadruped robots. *IEEE Robotics and Automation Letters*, 2(2):1023–1030, 2017.

[9] Xuxin Cheng, Yandong Ji, Junming Chen, Ruihan Yang, Ge Yang, and Xiaolong Wang. Expressive Whole-Body Control for Humanoid Robots, 2024. URL https://arxiv.org/abs/2402.16796.

[10] Arnaud Demont, Mehdi Benallegue, Abdelaziz Benallegue, Pierre Gergondet, Antonin Dallard, Rafael Cisneros, Masaki Murooka, and Fumio Kanehiro. The Kinetics Observer: A Tightly Coupled Estimator for Legged Robots, 2024. URL https://arxiv.org/abs/2406.13267.

[11] Kevin J. Doherty, Ziqi Lu, Kurran Singh, and John J. Leonard. Discrete-Continuous Smoothing and Mapping. *IEEE Robotics and Automation Letters*, 7(4):12395–12402, 2022. doi: 10.1109/LRA.2022.3216938.

[12] Sami Haddadin, Alessandro De Luca, and Alin Albu-Schäffer. Robot Collisions: A Survey on Detection, Isolation, and Identification. *IEEE Transactions on Robotics*, 33(6):1292–1312, 2017. doi: 10.1109/TRO.2017.2723903.

[13] Ross Hartley, Maani Ghaffari Jadidi, Lu Gan, Jiunn-Kai Huang, Jessy W Grizzle, and Ryan M Eustice. Hybrid Contact Preintegration for Visual-Inertial-Contact State Estimation Using Factor Graphs. In *Proceedings of the IEEE/RSJ International Conference on Intelligent Robots and Systems*, pages 3783–3790, 2018. URL https://arxiv.org/pdf/1803.07531.pdf.

[14] Ross Hartley, Josh Mangelson, Lu Gan, Maani Ghaffari Jadidi, Jeffrey M Walls, Ryan M Eustice, and Jessy W Grizzle. Legged Robot State-Estimation Through Combined Forward Kinematic and Preintegrated Contact Factors. In *Proceedings of the IEEE International Conference on Robotics and Automation*, pages 4422–4429, 2018. URL https://arxiv.org/pdf/1712.05873.pdf.

[15] Tairan He, Jiawei Gao, Wenli Xiao, Yuanhang Zhang, Zi Wang, Jiashun Wang, Zhengyi Luo, Guanqi He, Nikhil Sobanbab, Chaoyi Pan, Zeji Yi, Guannan Qu, Kris Kitani, Jessica Hodgins, Linxi "Jim" Fan, Yuke Zhu, Changliu Liu, and Guanya Shi. ASAP: Aligning Simulation and Real-World Physics for Learning Agile Humanoid Whole-Body Skills, 2025. URL https://arxiv.org/abs/2502.01143.

[16] Jemin Hwangbo, Carmine Dario Bellicoso, Péter Fankhauser, and Marco Hutter. Probabilistic foot contact estimation by fusing information from dynamics and differential/forward kinematics. In *2016 IEEE/RSJ International Conference on Intelligent Robots and Systems (IROS)*, pages 3872–3878, 2016. doi: 10.1109/IROS.2016.7759570.

[17] G.Yu. Kulikov and M.V. Kulikova. Accurate continuous–discrete unscented kalman filtering for estimation of nonlinear continuous-time stochastic models in radar tracking. *Signal Processing*, 139:25–35, 2017. ISSN 0165-1684. doi: https://doi.org/10.1016/j.sigpro.2017.04.002. URL https://www.sciencedirect.com/science/article/pii/S0165168417301305.

[18] Tzu-Yuan Lin, Ray Zhang, Justin Yu, and Maani Ghaffari. Legged robot state estimation using invariant kalman filtering and learned contact events. In Aleksandra Faust, David Hsu, and Gerhard Neumann, editors, *Proceedings of the 5th Conference on Robot Learning*, volume 164 of *Proceedings of Machine Learning Research*, pages 1057–1066. PMLR, 08–11 Nov 2022. URL https://proceedings.mlr.press/v164/lin22b.html.

[19] Michael Maravgakis, Despina-Ekaterini Argiropoulos, Stylianos Piperakis, and Panos Trahanias. Probabilistic Contact State Estimation for Legged Robots using Inertial Information. In *2023 IEEE International Conference on Robotics and Automation (ICRA)*, pages 12163–12169, 2023. doi: 10.1109/ICRA48891.2023.10161485.

[20] Marcel Menner and Karl Berntorp. Simultaneous State Estimation and Contact Detection for Legged Robots by Multiple-Model Kalman Filtering, 2024. URL https://arxiv.org/abs/2404.03444.

[21] K. P. Murphy. *Dynamic Bayesian Networks: Representation, Inference and Learning*. PhD thesis, University of California, Berkeley, 2002.

[22] J. Joe Payne, Daniel A. Hagen, Denis Garagić, and Aaron M. Johnson. Multi-Momentum Observer Contact Estimation for Bipedal Robots, 2024. URL https://arxiv.org/abs/2412.03462.

[23] Stylianos Piperakis, Michael Maravgakis, Dimitrios Kanoulas, and Panos Trahanias. Robust Contact State Estimation in Humanoid Walking Gaits. In *2022 IEEE/RSJ International Conference on Intelligent Robots and Systems (IROS)*, pages 6732–6738, 2022. doi: 10.1109/IROS47612.2022.9981354.

[24] Prashanth Ramadoss, Giulio Romualdi, Stefano Dafarra, Francisco Javier Andrade Chavez, Silvio Traversaro, and Daniele Pucci. DILIGENT-KIO: A Proprioceptive Base Estimator for Humanoid Robots using Extended Kalman Filtering on Matrix Lie Groups. In *2021 IEEE International Conference on Robotics and Automation (ICRA)*, pages 2904–2910, 2021. doi: 10.1109/ICRA48506.2021.9561248.

[25] Hilton Marques Souza Santana, João Carlos Virgolino Soares, Ylenia Nisticò, Marco Antonio Meggiolaro, and Claudio Semini. Proprioceptive State Estimation for Quadruped Robots using Invariant Kalman Filtering and Scale-Variant Robust Cost Functions. In *2024 IEEE-RAS 23rd International Conference on Humanoid Robots (Humanoids)*, pages 213–220, 2024. doi: 10.1109/Humanoids58906.2024.10769911.

[26] Sangli Teng, Mark Wilfried Mueller, and Koushil Sreenath. Legged Robot State Estimation in Slippery Environments Using Invariant Extended Kalman Filter with Velocity Update. In *2021 IEEE International Conference on Robotics and Automation (ICRA)*, pages 3104–3110, 2021. doi: 10.1109/ICRA48506.2021.9561313.

[27] Marco Tranzatto, Mihir Dharmadhikari, Lukas Bernreiter, Marco Camurri, Shehryar Khattak, Frank Mascarich, Patrick Pfreundschuh, David Wisth, Samuel Zimmermann, Mihir Kulkarni, Victor Reijgwart, Benoit Casseau, Timon Homberger, Paolo De Petris, Lionel Ott, Wayne Tubby, Gabriel Waibel, Huan Nguyen, Cesar Cadena, Russell Buchanan, Lorenz Wellhausen, Nikhil Khedekar, Olov Andersson, Lintong Zhang, Takahiro Miki, Tung Dang, Matias Mattamala, Markus Montenegro, Konrad Meyer, Xiangyu Wu, Adrien Briod, Mark Mueller, Maurice Fallon, Roland Siegwart, Marco Hutter, and Kostas Alexis. Team CERBERUS Wins the DARPA Subterranean Challenge: Technical Overview and Lessons Learned, 2022. URL https://arxiv.org/abs/2207.04914.

[28] Yibin Wu, Jian Kuang, Shahram Khorshidi, Xiaoji Niu, Lasse Klingbeil, Maren Bennewitz, and Heiner Kuhlmann. DogLegs: Robust Proprioceptive State Estimation for Legged Robots Using Multiple Leg-Mounted IMUs, 2025. URL https://arxiv.org/abs/2503.04580.

[29] Yufei Xue, Wentao Dong, Minghuan Liu, Weinan Zhang, and Jiangmiao Pang. A Unified and General Humanoid Whole-Body Controller for Versatile Locomotion, 2025. URL https://arxiv.org/abs/2502.03206.

[30] Shuo Yang, Howie Choset, and Zachary Manchester. Online Kinematic Calibration for Legged Robots. *IEEE Robotics and Automation Letters*, 7(3):8178–8185, 2022. doi: 10.1109/LRA.2022.3186501.

[31] Shuo Yang, Zixin Zhang, Benjamin Bokser, and Zachary Manchester. Multi-IMU Proprioceptive Odometry for Legged Robots. In *2023 IEEE/RSJ International Conference on Intelligent Robots and Systems (IROS)*, pages 774–779, Detroit, MI, USA, October 2023. IEEE. ISBN 978-1-6654-9190-7. doi: 10.1109/IROS55552.2023.10342061.

[32] Donghoon Youm, Hyunsik Oh, Suyoung Choi, Hyeongjun Kim, Seunghun Jeon, and Jemin Hwangbo. Legged Robot State Estimation with Invariant Extended Kalman Filter Using Neural Measurement Network. In *2025 IEEE International Conference on Robotics and Automation (ICRA)*, pages 670–676, 2025. doi: 10.1109/ICRA55743.2025.11127971.

[33] Kevin Zakka, Baruch Tabanpour, Qiayuan Liao, Mustafa Haiderbhai, Samuel Holt, Jing Yuan Luo, Arthur Allshire, Erik Frey, Koushil Sreenath, Lueder A. Kahrs, Carmelo Sferrazza, Yuval Tassa, and Pieter Abbeel. MuJoCo Playground, 2025. URL https://arxiv.org/abs/2502.08844.